

MODELING, ANALYSIS AND AUTOPILOT DESIGN FOR AN AIRSHIP

A. A. Pashilkar*

Abstract

In this paper a flight dynamic model of an airship is described. This model is used for flight mechanics analysis. A heading autopilot design has been implemented for the airship.

Nomenclature

C_L, C_D, C_m, C_l	= aerodynamic coefficients (lift, drag, pitching moment, rolling moment, yawing moment and side force)
\bar{f}	= vector equations of motion
p, q, r	= body axis rates, rad/s
t	= time, sec
u, v, w	= body axis velocities, m/s
X, Y, H	= components of the inertial distance of the aircraft, m
\bar{x}	= vector of states
\bar{u}	= vector of control inputs
V	= mean velocity in the tunnel, m/s
l	= length of the airship, m

Greek Symbols

α	= angle of attack, rad
β	= angle of sideslip, rad
$\delta_p, \delta_e, \delta_\alpha, \delta_r$	= throttle (percent), elevator (rad), aileron (rad), rudder (deg)
ψ, θ, ϕ	= euler angles, rad

Introduction

There is a renewed interest at home [1] and abroad [2] in the area of airship design and development. This is due to their potential application in varied tasks such as surveillance, advertising, monitoring, inspection, exploration and research roles (Refs. 4- 6). In the country, Gazder and Pant [7] have examined the feasibility of using airships for passenger transport in comparison to helicopters in hilly terrain. These studies indicate cost benefits arising due to the use of airships in civilian applications. In many of the applications like surveillance, environmental monitoring, advertising etc., it is more appropriate to consider the use of a remotely controlled vehicle.

Considering the interest in this area of design, it is appropriate to examine the flight dynamics and control of remote controlled airships [2,9]. Fig.1 shows a sketch of the proposed airship. It consists of an envelope with a wankel engine mounted at the bottom. The aerodynamic fins are mounted behind in an inverted 'Y' configuration. There are control surfaces on the fins driven by servomotors. Ballonets inside the airship will be used to control the net buoyancy.

This paper discusses the mathematical modeling and heading autopilot control design of a remote blimp (i.e., an airship whose envelope is structurally supported by internal buoyant gas pressure). The modal characteristics of the dynamics are discussed with relevance to the control system design issues.

Aerodynamics and Inertia

Reference 2 presents the development of the equations of motion of an airship. The basic derivation is based on the rigid body equations of motions used routinely in fixed wing aircraft simulation. Notable differences arise in the considerations of buoyancy and the apparent mass of the airship. The apparent mass of an airship is the additional mass of air that it displaces due to motion in the atmosphere. Calculations for ellipsoidal shapes are due to Lamb [10] in the form of inertia coefficients.

The data used in this paper has been generated for an aerostat configuration ($l/d = 3.0$) in static [11] and dynamic [12] wind tunnel tests. The present airship has a l/d value of 3.2 which is sufficiently close to the aerostat. The final shape is likely to be different but may not cause a significant effect on the aerodynamic derivatives. A summary of the static and dynamic derivatives used for simulation and control design are presented in Table-1.

* Scientist, Flight Mechanics and Control Division, National Aerospace Laboratories, Post Box No. 1779, Bangalore-560 017, India
Manuscript received on 28 Dec 2002; Paper reviewed, revised and accepted on 13 Jun 2003

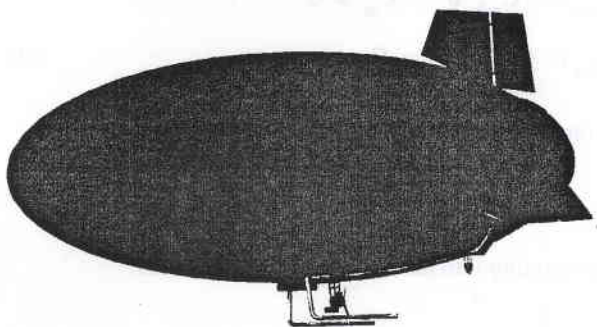


Fig. 1 Schematic of the remote controlled blimp

The mass and inertia properties of the airship have been assumed as per the estimates of the design group at NAL. The properties are listed in Table-2. The engine performance for the remote airship is taken as a maximum thrust of 560N at all altitudes up to 3 kms.

Based on the data assumed, it is seen that the ceiling altitude for this airship is 1200m in ISA conditions at low speeds. At higher speeds, the envelope generates some lift, which can be used to increase the ceiling altitude close to 1500m.

Mathematical Model

The dynamic equations of motion of the airship are usually written about the center of buoyancy (Ref. 2). In this form the apparent mass effect due to the large volume of the air mass displaced is included. Further, the effect of venting or intake of ballast air results in a change in the

Table-1 : Aerodynamic Derivatives (1/deg) about Envelope Fixed Axis	
Longitudinal	
C_{L0}	0.0
C_{La}	0.02
C_{Lq}	-0.0004188
C_{Lde}	0.0012
C_{D0}	0.06
C_{Da^2}	0.0055
C_{m0}	0.0
C_{ma}	-0.027
C_{mq}	-0.0002094
C_{mde}	-0.0006
Lateral-directional	
$C_{Y\beta}$	-0.0300
C_{Ydr}	0.00142
C_{Yda}	0.00005516
$C_{l\beta}$	-0.0000009
C_{lp}	-0.000029668
C_{ldr}	0.0001178
C_{lda}	-0.00001842
$C_{n\beta}$	0.00087
C_{nr}	-0.0023
C_{ndr}	-0.00071
C_{nda}	-0.00001493
<i>Note : Derivatives not presented above are taken as zero</i>	

Table-2 : Mass and Inertia Properties
Envelope mass = 107.000 kgs
Gondola mass = 112.000 kgs
Density of Helium = 0.170 kg/m ³
Envelope Interias :
$I_x = 118.120 \text{ kgm}^2$
$I_y = 2886. \text{kgm}^2$
$I_z = 2886.200 \text{ kgm}^2$
$I_{xy} = 0.000 \text{ kgm}^2$
$I_{yz} = 0.000 \text{ kgm}^2$
$I_{zx} = 0.020 \text{ kgm}^2$
Apparent Inertia Coefficients
$k_1 = 0.122$
$k_2 = 0.803$
$k_p = 0.465$
C.G. Location of Envelope
X-direction 7.541m from envelope nose
C.G. Location of Gondola/Engine
X-direction 7.541m from envelope nose
Y-direction 0.000m from envelope nose
Z-direction 2.758 downward from envelope nose

position of the center of gravity of the airship which gives rise to additional terms in the equations of motion (Ref. 3). In this paper two simplifications are proposed.

First, consider the effect of venting or taking in ballast air into the ballonets. This activity will be undertaken during the ascent or descent phase of the airship and rarely during maneuvering. It is the latter that is of interest in this paper. Also the magnitude of the forces introduced due to such activity is small (a 5kg/s gas discharge issuing with a velocity of 3m/s relative to the airship results in a 15N force). The rate of change of center of gravity is also neglected as it results in a c.g. travel rate of approximately $(5\text{Kg/s} * 1.5\text{m}) / 200 \text{ Kg} = 0.037\text{m/s}$ lasting for about $40\text{kg} / 5\text{kg/s} = 8$ seconds at the most. Thus, in summary, one may determine the center of gravity as it changes and translate all the forces, moments and inertias to this point to calculate the dynamics, resulting in the standard form of the six-degree-of-freedom equations.

$$\begin{aligned} \dot{\bar{x}} &= \bar{f}(\bar{x}, u) \\ \bar{x} &= [u, v, w, p, q, r, \psi, \theta, \phi, X, Y, H] \\ \bar{u} &= [\delta_p, \delta_e, \delta_a, \delta_r] \end{aligned} \tag{1}$$

This is in contrast to the approach used in Ref. 2 where the equations are written about the center of buoyancy. The equations in this paper have been written about the center of mass. This change is accomplished in two steps

- center of mass location in body fixed coordinates is calculated every time
- moment of inertias of the components like gondola and envelope are translated to the center of mass.

This allows us to uncouple the accelerations and write the equations of motion in the conventional form (1). Nevertheless, it is important to retain the different apparent mass values along the three linear directions as calculated using Lamb's coefficients [10] for the ellipsoid. Linearization of the equations results in the modal characteristics of the blimp. Since the states X, Y and ψ do not couple into the rest of the equations, the resulting linear model is a 9th order system (longitudinal states: u, w, q, θ, H , lateral states : v, p, r, ϕ).

The static balance characteristics of the blimp are of interest in understanding the control issues. Consider the pitching moment and lift balance equations at aerodynamic derivative level.

$$\begin{aligned} C_{m\alpha} \alpha + C_{m\delta e} \delta_e &= C_m = 0 \\ C_{L\alpha} \alpha + C_{L\delta e} \delta_e &= C_L \end{aligned} \tag{2}$$

From the first of the above equations we have

$$\alpha_{trim} = -\frac{C_{m\delta e} \delta_{e_{trim}}}{C_{m\alpha}} \tag{3}$$

Substituting into the lift equation one obtains

$$C_L = \left[C_{L\delta e} - C_{L\alpha} \frac{C_{m\delta e}}{C_{m\alpha}} \right] \delta_{e_{trim}} \tag{4}$$

It is seen that the first term in parenthesis is the lift increment due to the elevator deflection alone, while the second term is that due to the an increase in angle of attack. Using the derivative values in Table-1, one obtains

$$C_L = 7.56 \times 10^{-4} \delta_{e_{trim}} \tag{5}$$

This means that in order to climb, the elevator deflection must be positive (trailing edge down). This is contrary to the behavior of a conventional aircraft where one needs to deflect the elevator trailing edge up to climb. The reason for this is that in the latter, the up elevator causes, the aircraft to pitch up and the angle of attack to increase. Increase of angle of attack generates lift from the wings, which is far in excess of the downward lift due to the elevator. Since, in an airship there are no wings, the lift due to elevator dominates. One may therefore conclude that the elevator reversal from conventional fixed wing response to the airship type occurs when

$$C_{L\delta e} > C_{L\alpha} \frac{C_{m\delta e}}{C_{m\alpha}}$$

It has been pointed out in Ref. 4 that the airships tend to show non-minimum phase behavior in altitude with elevator deflection. A non-minimum behavior is associated with a right half zero in the transfer function. This is typical of all fixed wing aircraft altitude to elevator transfer function at low speeds (back side of the drag polar). In case of the airship, this characteristic is found through out the speed range.

The climb performance of the airship is different from a conventional aircraft. The force balance equations in a climb are given by:

$$\begin{aligned} T - D + (B - W) \sin \gamma &= 0 \\ L + (B - W) \cos \gamma &= 0 \end{aligned} \tag{6}$$

Where, B is the buoyancy force on the airship, W is the weight, T is the engine thrust, D is the drag, L is the lift and γ is the flight path angle. The first equation above describes the balance of forces in the direction of the flight path. If this is disturbed, the velocity will either increase or decrease. The other equation describes the force balance perpendicular to flight path. When this equation is not satisfied, the airship flight path will begin to change (curve up or down). For an airship, the net buoyant force ($B-W$) is positive when it is climbing. The airship can be made to climb using the buoyancy force of the lighter gas in the envelope (vertical ascent). However, a faster climb results by using the engine thrust set at maximum. The above discussion shows that the buoyancy will aid the thrust force during a climb. Also the lift force has to be negative to balance the second equation. The angle of attack can be reduced with the help of down elevator. The typical angle of attack of this airship is less than half a degree. At higher angles of attack the drag increase is high and the additional lift increase is marginal.

It is interesting to compare the performance with that of a conventional aircraft. This is seen by replacing ($B-W$) in eqn. (6) with $-W$.

$$\begin{aligned} T - D - W \sin \gamma &= 0 \\ L - W \cos \gamma &= 0 \end{aligned} \tag{7}$$

Increase in velocity for a conventional aircraft will result in increased drag and therefore to compensate, the angle of attack must be reduced. This will result in a decrease in flight path angle because the left hand side of the second equation will become negative causing the flight path to curve downward. Since climb rate is a given by $V \sin \gamma$, there is a combination of airspeed and flight path angle which will give fastest climb.

In the above analysis, the moment balance equation has been ignored. In case of an airship, the engine is mounted below the envelope and it generates a pitch up moment when thrusting. Considering that the engine is vertically below the center of gravity of the entire vehicle, tilting the engine will result in a decrease of the thrust along the flight path and also reduce the pitch up moment due to the engine. Further, the thrust will have a component in the direction of the buoyancy force. The net result of tilting the engine upward is to cause the airship speed and the angle of attack to reduce in order to maintain a steady climb. Therefore, there is no significant advantage of tilting the engine upward in this case. Tilting the engine downward will however be useful to increase the rate of

descent. The vectoring of the engine in yaw is also not useful because, the proximity of the engine to the center of gravity makes it inefficient for yawing the airship. At low speeds however, a yaw thruster mounted on the tail plane can be beneficial for maneuvering.

Modal Characteristics

In Fig.2, the modal characteristics of the airship are presented. These have been obtained by linearization of the equations of motion of the airship at different air speeds (5m/s to 20m/s in steps of 5m/s) for a fixed altitude of 50 meters. The overall modes and their relative characteristics do not change with altitude. The trim conditions have been calculated using the ballonnet mass to balance altitude, the angle of attack to balance the pitching equation and the engine thrust to balance the drag. The ballonnet mass required to trim at different speeds and altitudes is shown in Fig.3. The corresponding values of the trim angle of attack are plotted in Fig.4. It is seen that the altitude has negligible effect on the trim angle of attack. A summary of the modal characteristics is given below:

Longitudinal Modes

Pitch Pendulum: Stable oscillatory with low damping. This is due to the effect of the center of gravity being below the center of buoyancy. The distance between these two points determines the natural frequency of this mode at low frequencies. As the speed increases the aerodynamic forces become more dominant. This results in an increase in the frequency of the pitch mode.

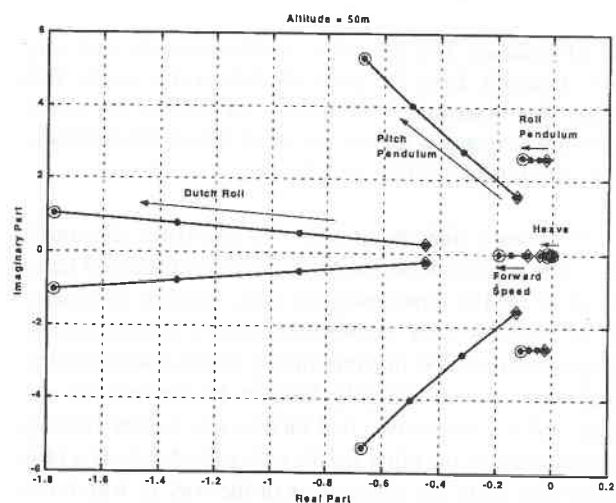


Fig. 2 Modal characteristics of the blimp

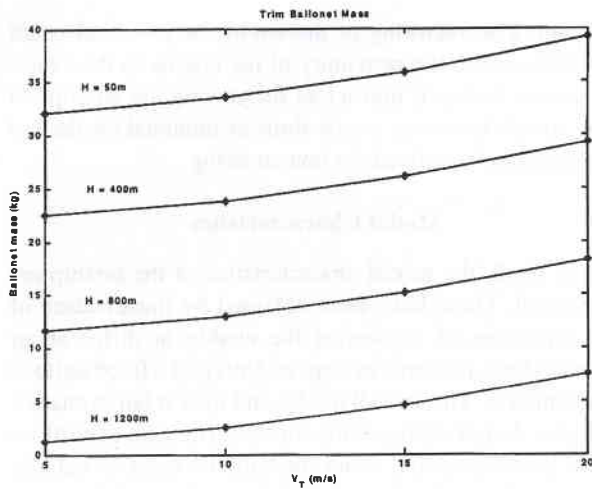


Fig. 3 Ballonet mass required to trim at various speeds and altitudes

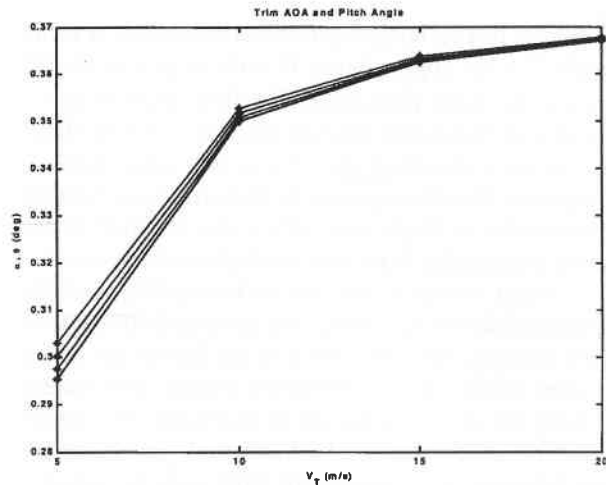


Fig. 4 Trim angle of attack as a function of speed for various altitudes

Heave Mode : At low speeds two real stable poles represent this mode. As the speed increases these two stable poles combine to form an oscillatory mode with high damping.

Forward Speed: This mode is always a stable real mode. Unlike a conventional fixed wing aircraft, the coupling between forward speed and heave mode is missing. This means that there is no mode equivalent to the phugoid in case of the airship.

Lateral-directional Modes

Dutch Roll: This mode is stable and oscillatory with high damping. It combines sideslip with the yawing motion. The natural frequency of this mode increases with speed.

Roll Pendulum: This is a stable oscillatory mode with very low damping. Like the pitch pendulum this mode also arises due to metacenteric height. Increase of the speed does not have any effect on this mode due to the relatively low aerodynamic forces in roll.

It is seen that the modal characteristics discussed above is applicable to the airship model discussed here. Cook et. al [9] have analyzed other airships in greater detail and they show somewhat different characteristics. In particular we note that this airship model shows a Dutch Roll mode, which is highly damped. In contrast, the airship in Ref.9 shows two real modes, one for the sideslip subsidence and the other for the yaw subsidence. It is also noted that there are differences in the way in which the natural frequency and damping of the pitch pendulum mode changes with airspeed. It is clear that these differ-

ences arise due to the particular values of the derivatives used in this paper.

Yaw Autopilot Design

A guidance control system for the remote blimp has been described in Ref.8. The inner loop of this controller is a heading control system. In this section the heading controller design is discussed. The dynamics indicates that the rudder is the most effective control surface for achieving heading control. The overall scheme of the heading controller is shown in Fig.5. There are two feedback loops. The heading hold loop consists of a proportional feedback from the heading angle to the rudder. The roll rate is feedback is intended to damp the resulting roll oscillations arising due to the lightly damped roll pendulum mode. A proportional gain is sufficient for the heading controller as

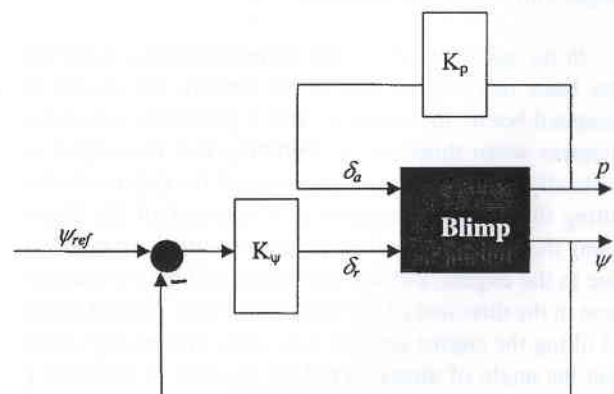


Fig. 5 Heading controller scheme

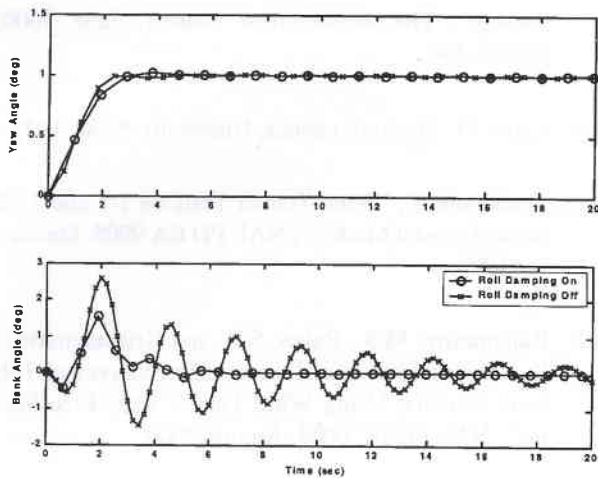


Fig. 6 Heading controller response with and without roll damping ($V=20\text{m/s}$)

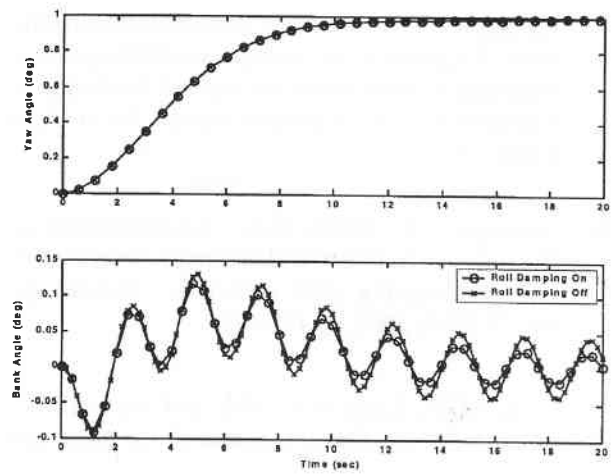


Fig. 7 Heading controller response with and without roll damping ($V=5\text{m/s}$)

the plant acts as an integrator assuring good steady state characteristics.

The maximum deflection of the rudder is ± 25 degrees. The K_{ψ} ($= -1.67$ deg/deg) gain has been chosen so that rise time is in the range of 2 to 5 seconds and the rudder does not reach position limits for heading errors less than about 15 degrees. The roll damping gain is chosen as $K_p = 6$ deg/deg/s again to ensure that the resulting roll oscillations are damped out without the aileron surfaces reaching their position limits. Fig.6 shows the response of the heading controller at 20m/s. The same controller at 5m/s has a response shown in Fig.7. At higher speeds the system responds faster to a yaw command and also there appears to be some advantage in having the roll damping on. The actuator model has not been considered in this analysis on the assumption that its bandwidth is much higher than the closed loop bandwidth of this design. A composite delay of 100milliseconds has been taken to account for the digital controller delays arising from update rate and analog to digital conversion.

Conclusions

A six-degree-of-freedom model of the blimp has been developed using available data. The dynamic modes have been computed throughout the flight envelope. A heading controller with proportional gain has been designed as the inner loop of the autopilot.

Acknowledgements

The author would like to thank Mr S. Selvarajan, NTAF, NAL for the data used in this paper.

References

1. Amol, G. and Pant, R.S., "Design, Fabrication and Flight Testing of Remotely Controlled Airship", Presented at the National Workshop on Lighter-than-air Technologies, October 30-31, Agra Cantt, 2002.
2. Khoury, G.A. and Gillett, J.D., Eds. Airship Technology, Cambridge Aerospace Series : 10, ISBN 0 521 430 747, Cambridge University Press, 1999.
3. An, J., Yan, M., Zhou, W., Sun, X. and Yan, Z., "Aircraft Dynamic Response to Variable Wing Sweep Geometry", Journal of Aircraft, Vol.25, No.1, March 1988, pp.216-221.
4. Elfes, A., Bueno, S.S., Bergerman, M. and Ramos, J.G., "A Semi-autonomous Robotic Airship for Environmental Monitoring Missions", Proceedings of the IEEE International Conference on Robotics and Automation, May 1998, pp.3449-3455.
5. Barter, G., Burton, R, et.al., Final Design Report LTAV Design Team, Massachusetts Institute of Technology, Department of Aeronautics and Astronautics, May 16,2002.
<http://web.mit.edu.ktdunn/Public/82/report.pdf>.
6. Seeman, G.R., Harris, G.L., Brown, G.J. and Cullian, C.A., "Remotely Piloted Mini-Blimps for urban Applications", Astronautics and Aeronautics, February 1974, pp.31-35.

7. Gazder, R.P. and pant, R.S., "A Comparative Evaluation of Operation of Airships and Helicopters in Uttaranchal", Presented at the National Workshop on Lighter-than-air Technologies, October 30-31, Agra Cantt, 2002.
8. Azinheira, J.R., Paiva, .et.al., "Lateral/Directional Control of an Autonomous Unmanned Airship", Aircraft Engineering and Aerospace Technology, Vol.73, No.5, 2001, pp.453-458.
9. Cook, M.V., Lipscombe, J.M. and Goineau, F., "Analysis of the Stability Modes of the Non-rigid Airship", The Aeronautical Journal, June 2000, pp.279-290.
10. Lamb, H., Hydrodynamics, University Press, 1932.
11. Sundaram, S., "Wind Tunnel Tests on 1:7 and 1:28 Scale Aerostat Models", NAL PD EA 9905, December 1999.
12. Rajamurthy, M.S., Rajan, S.R. and Krishnamurthy, K., "Determination of Dynamic Derivatives of 160 cu.m Aerostat Using Wind Tunnel Semi-Free Flying", NAL PD FC 0004, August 2000.